doi.org/10.36721/PJPS.2024.37.4.REG.839-847.1

Agrimonia pilosa ledeb alleviates inflammatory responses in diabetic kidney disease by inhibiting the JNK/p38 signaling pathway

Zhi Liu*, Wenxing Hu and Yanhui Li
Endocrinology Department of Qingbaijiang District People's Hospital, Chengdu City, China

Abstract: Inflammatory response is a key for the emergence and progression of diabetic kidney disease (DKD). Studies have proved that *Agrimonia pilosa* Ledeb (APL) as a traditional Chinese herbal medicine has strong anti-oxidant and anti-inflammatory effects, but how APL plays on DKD hasn't been reported. This work explored the effects and potential regulatory mechanism of APL in DKD, aiming to inspire new ideas for developing novel drugs for DKD. DKD mice were induced by streptozotocin (STZ) and treated with APL extract of different concentrations by gavage. Blood glucose, blood lipids, renal function, and histopathological examination were performed using blood glucose meter and biochemical analyzer, HE staining, PAS staining and immunohistochemistry separately. Subsequently, Western blot and ELISA were used to determine the expression of inflammatory factors and JNK/p38 pathway proteins in mice kidney tissue. The results showed that APL concentration-dependently reduced blood glucose and lipid levels in DKD mice, alleviated kidney injury, and reduced the expression of fibrotic factors and inflammatory factors in kidney tissue. In addition, APL also effectively inhibited the expression of the JNK/p38 pathway proteins. It can be speculated that APL may alleviate pathological damage and inflammatory response in DKD by inhibiting the JNK/p38 signaling pathway.

Keywords: APL, DKD, inflammatory response, JNK/p38 signaling pathway

INTRODUCTION

Representing the foremost vascular long-term complication of diabetes, DKD (namely diabetic kidney disease) is the predominant cause of end-stage kidney disease worldwide (Samsu, 2021; B. Zhang *et al.*, 2021), affecting approximately 15-40% of individuals with diabetes. The primary characteristics of DKD include glomerular atrophy and accumulation of extra cellular matrix, which deteriorate renal structure and function (Piccoli *et al.*, 2015). In clinical presentations, DKD is characterized by ongoing proteinuria, diminished renal function and elevated blood pressure. The primary treatment for DKD involves medications that control hyperglycemia, dyslipidemia and hypertension, or inhibit the renin-angiotensin-aldosterone system (Ahmad, 2015; Tang *et al.*, 2021). However, the currently-approved synthetic drugs often come with side effects, which may also result in end-stage kidney disease (Johnson and Spurney, 2015). This circumstance necessitates seeking more safe and effective alternatives for treating this disease.

Chinese herbal medicines, derived from natural plants and with minimal industrial processing, have been used in the long run for treating a variety of diseases by virtue of their safety (Tang *et al.*, 2021). *Agrimonia pilosa* Ledeb (referred to as APL), a perennial herbaceous plant, contains such key components as isocoumarins, tannins, triterpenes, organic acids, phloroglucinol derivatives and flavonoids (S. B. Kim *et al.*, 2017; T. Jin *et al.*, 2022). Traditionally, APL is employed in treating such conditions as sore throat, eczema, parasitic infections, abdominal pain, headache and bloody secretions (Wen *et al.*, 2022). Pathologically, APL can help the body resist tumors, viruses, inflammation, oxidation, fatigue and hyperglycemia (Santos *et al.*, 2017; C. Y. Kim *et al.*, 2020; T. Jin *et al.*, 2022). As proved in existing articles, APL can suppress inflammatory responses by dampening the expressions of inflammatory factors, inducible nitric oxide synthase and reactive oxygen species (Bae *et al.*, 2010; Jung *et al.*, 2010). It can also enhance coagulation function and lower blood sugar activity by holding up the inflammatory responses in rats on a high-fat diet (Jang *et al.*, 2017). This anti-inflammatory mechanism is attributable to APL's suppression of the JNK/p38 MAPK signaling pathway (X. Jin *et al.*, 2016), while the role and mechanism of APL in DKD are unclear.

A primary contributor to the onset and growth of DKD is inflammation (Perez-Morales *et al.*, 2019). As two classic MAPK signaling pathways, p38 MAPK and JNK can be triggered by a hyper blood sugar level, intervening in tissue inflammation and cellular apoptosis (Sanchez and Sharma, 2009). If activated in the kidneys of DKD patients, JNK/p38 MAPK may release transforming growth factor (TGF)-β1 and the like inflammatory mediators, causing inflammatory damage to kidneys and ultimately resulting in glomerulosclerosis and renal fibrosis (Y. Zhang *et al.*, 2018). Hence, an effective way to prevent and control DKD is to alleviate inflammation by stopping the activation of JNK/p38 MAPK.

APL is anti-inflammatory, whereas, it is not definite whether APL affects DKD. In this context, the author

**Corresponding author:* e-mails: ziyi39406791@163.com

hypothesized that APL functioned in treating DKD and this functioning might be linked to the JNK/p38 MAPK signaling pathway. In this work, DKD animal models were created by induction using Streptozotocin (STZ), followed by detecting the pathological indicators of kidneys and the expressions of JNK/p38 MAPK pathway proteins in DKD mice. The objectives were to understand the therapeutic mechanism of APL in DKD mice and assess the potential of using APL, instead of synthetic drugs, for treating DKD.

MATERIALS AND METHODS

Modeling and grouping for experiment

For this work, 24 mice numbered C57BL/6J, aged 6-8 weeks and weighed 20-23 g, were obtained from Silaike (Shanghai, China). All animal experiments were approved by the Ethics Committee of Qingbaijiang District People's Hospital and conducted per the guidelines for the welfare and use of experimental animals. APL powder extract was procured from Selleck Chemicals (Houston, TX, USA) and stored at -20°C. The mice were bred as per the rules for experimental animal feeding under the following conditions: 22-25°C (room temperature), 60% (humidity), free access to water and food, and alternated cycle of 12 h with light and 12h in the dark. After one week of accommodation, the mice received an intraperitoneal injection of STZ (S8050, manufacturer, Solarbio, Beijing, China) and uninephrectomy to form DKD animal models as detailed below: The mice were anesthetized and exposed the left kidney through a dorsal incision, then excised after ligating the renal pedicle with 4/0 surgical suture. One week after the uninephrectomy, the mice received STZ (dissolved in 0.1mol/L citrate buffer) by intraperitoneal injection for 50mg/kg/d lasting for 5 days. One week later, blood samples were collected from the mice's tail veins, and fasting blood glucose (FBG) level was determined using a blood glucose meter (Roche, Basel, Switzerland). If the FBG level exceeded 16.7 mmol/L, it was confirmed that these DKD mice models were created successfully and could be used for subsequent studies.

The successfully modeled mice were classified into the control group (Con group), model group (STZ group), low-dose APL group (STZ+APL-L group) and high-dose APL group (STZ+APL-H group), with 6 mice in each group. After FBG level detection to confirm successful modeling, the STZ+APL-L group and STZ+APL-H group were intragastrically administered with APL of 100 mg/kg and 200mg/kg respectively. The Con group and STZ group were intragastrically administered with normal saline. This administration was performed once a day and continued for 12 weeks. Twelve hours after the last administration, various indicators were tested.

The blood glucose and blood lipid levels determination

Twelve hours after the final administration and subsequent fasting, the author collected the mice's tail vein blood and tested the blood glucose and blood lipid levels using a glucometer and an automatic biochemistry analyzer (BS-2800M, Mindray, Shenzhen, China). The testing indicators involved the levels of hemoglobin A1c (HbA1c), the FBG, the triglyceride (TG), the total cholesterol (TC) and the low-density lipoprotein (LDL).

Renal function determination

After the last administration to the mice, the urine samples were collected using metabolic cages over 24 hours. Recorded the mice's body weight (BW), then anesthetized the mice with 1% pentobarbital sodium (5 ml/kg of body weight) through intraperitoneal injection, collected the blood from the left femoral artery of the mice, serum was separated by placing the blood at 37°C for 1 hour and centrifuging at 3000 r/min for 10 minutes. The collected urine and serum were tested using an automatic biochemistry analyzer to acquire the contents of blood urea nitrogen (BUN), serum creatinine (Scr), and urinary albumin excretion (UAE) of the mice. After euthanasia, the kidneys were excised, weighed and stored at -80°C for histopathological analysis. Fig. out the Kidney index (kidney weight/body weight, KW/BW).

Histopathological test

The renal tissue samples were dipped in 4% paraformaldehyde (441244, Sigma Aldrich, St. Louis, MO, USA) overnight for fixation. After being dehydrated, the fixed tissues were embedded in paraffin and sectioned into thin slices (4μm/slice). The slices were dyed with hematoxylin-eosin (HE) for the histopathological conditions of kidneys in mice, periodic acid-Schiff (PAS) staining for glycogen deposition and α-smooth muscle actin (α-SMA) staining was implemented to examine the expression of fibrotic protein. The histopathological conditions of the groups were checked under a microscope (BX51, Olympus, Tokyo, Japan).

HE Staining

The slices of renal tissue were put in xylene (1330-20-7, Nanjing Reagent, Nanjing, China) for dewaxing. Then, the slices were cleaned with water, and dehydrated by gradient concentrations of ethanol, followed by 3-5 minutes with hematoxylin (C0107, Beyotime, Shanghai, China). The slices were immersed in a 1% acidic alcohol solution containing 70% hydrochloric acid for a while for differentiation and cleaned with running water, followed by bluing with 1% ammonia-water solution for a moment and rinsing, staining in a solution with 0.5% eosin (G1100, Solarbio) for 3 minutes. After gradient ethanol dehydration(with 70% ethanol for 1 minute, 80% ethanol for 1 minute, and 95% ethanol for 10 minutes, and dehydrate 3 times with anhydrous ethanol for 20 minutes each), xylene transparency and neutral resin (G8590, Solarbio) encapsulation, the slices were put under a microscope to monitor the pathological changes in the kidneys.

PAS Staining

After dewaxing and ethanol-based dehydration, the renal tissue slices were rinsed using distilled water, then dyed with a staining solution of Alcian Blue (G1560, Solarbio) for 10-20 minutes and washed three times with distilled water (1-2 minutes for each time of washing). After that, the slices were oxidized in an oxidizing solution for 5 minutes and washed twice with distilled water, stained in a PAS staining solution (C0142S, Beyotime) for 10-20 minutes in the dark and then washed with running water for 10 minutes, stained with a hematoxylin solution for 1-2 minutes and then rinsed with water, blued for 3 minutes in Scott's bluing solution (G1865, Solarbio) and then cleaned with water in succession. After gradient ethanol dehydration, xylene transparency and neutral resin encapsulation, observed the presence of glycogen and other PAS-positive substances in the tissues under a microscope.

Immunohistochemical assay on α-SMA

After dewaxing and hydration, antigen repair was performed with citrate antigen repair solution (C1032, Solarbio), then blocked with avidin/biotin blocking buffer (C-0005, HaoRan Biotech, Shanghai, China) at room temperature and then sealed for 30 minutes with 3% BSA. Sections were incubated overnight with rabbit anti-α-SMA (1:200, ab232784, Abcam, Waltham, MA, USA) primary antibody at 4°C and then with sheep anti-rabbit secondary antibody (1:500, ab150077, Abcam) for 1 h at 37℃. Afterward, the slices were dyed by streptavidin-horseradish peroxidase complex (OR03L, Sigma-Aldrich) for 20 minutes at 37°C, followed by image developing using Pierce DAB substrate kits (24002, Thermo Scientific, Waltham, MA, USA). The next was to counter-stain the slices with hematoxylin for 5 minutes, After gradient ethanol dehydration, xylene transparency and neutral resin encapsulation, observed and photographed the renal tissue slices under a microscope.

Western Blot assay

Kidney tissue samples were maintained in pre-chilled lysis buffer (20101ES60, Yeasen Biotechnology, Shanghai, China) at 4°C for 30 minutes to extract protein. 20μg protein sample was separated using 10% SDS-PAGE (namely sodium dodecyl sulfate-polyacrylamide gel electrophoresis), then, transferred the protein to PVDF (i.e., polyvinylidene difluoride) membrane which was blocked for 1 hour at room temperature in a 0.2% TBST (tris buffered saline with tween 20) buffer containing 5% defatted milk. After that, the membrane got cleaned and respectively incubated with the following primary antibodies sourced from Abcam for one night in a setting of 4°C: rabbit anti-TGF-β (1:1000, ab215715), α-SMA (1:500, ab232784), collagen I (1:1000, ab260043), fibronectin (1:1000, ab268020), IL-1β (1:1000, ab254360), TNF-α (1:1000, ab183218), IL-6 (1:1000, ab259341), p-JNK (1:1000, ab124956), JNK (1:1000, ab179461), p-p38 (1:1000, ab4822), p38 (1:1000, ab101840), p-ERK (1:1000, ab201015) and ERK (1:1000, ab229912), with GAPDH (1:2500, ab9485) serving as the internal reference protein. Thereafter, the solution of the primary antibody was discarded, and the membrane was washed using TBST. Further, the membrane was dosed with goat anti-rabbit IgG (1:2000, ab6721) for 30 minutes of culture at room temperature. After being washed with TBST again, the membrane was applied with an ECL solution (P0018S, Beyotime) for color development and exposure. Chemiluminescent Imaging Analysis System (5200, Tanon, Shanghai, China) was used to capture the protein strips and Image J 1.8.0 software (designed by the National Institutes of Health, Bethesda, MD, USA) was to assess the grayscale value of each protein strip.

ELISA assay

The ELISA, namely enzyme-linked immunosorbent assay, tested the inflammatory factors in tissue homogenate of kidney. The kidney samples were homogenized on ice using mixer and disrupted ultrasonically, centrifuging for 10 minutes at 4°C to collect the supernatant and the kits (PI301, PT512 and PI326, Beyotime, Shanghai, China) were used to examine the concentrations of IL-6, TNF-α, and IL-1β as per the operation instruction.

Ethical approval

This study was approved by the Ethics Committee (HGB-202304085) of Qingbaijiang District People's Hospital, China.

STATISTICAL ANALYSIS

In this work, the data analysis was based on the SPSS 26.0 software designed by SPSS Inc., Chicago, IL, USA and graphs were plotted using the GraphPad Prism 9.0 software designed by GraphPad Inc., La Jolla, CA, USA. Two groups were compared with the t-test method; multiple groups were compared with the one-way ANOVA method; subsequently, Tukey's post-hoc analysis was applied. All data are recorded as mean ± standard deviation. For all analyses, where $*P<0.05$, $**P<0.01$, $***P<0.001$ and $****P<0.0001$ are shown, it means that the corresponding datas are statistically significant.

RESULTS

APL-based Improvement in the Blood Glucose and Lipid Levels of DKD mice

Twelve hours after the final administration, various indicators were measured. Compared to the control group, the FBG level in the STZ group was elevated greatly, exceeding 16.7mmol/L, representing the successful establishment of DKD animal models. Compared to the STZ group, APL functioned well in alleviating blood glucose, especially for the high dose of APL (200 mg/kg): in the STZ+APL-H group, the mice experienced a

pronounced drop in FBG and HbAlc levels (P<0.05), figs. 1A-1B). APL also caused a decline in the contents of TC, TG and LDL in DKD mice, demonstrating a certain regulatory effect on blood lipid metabolism (figs. 1C-1E). The measured results indicate that APL alleviated the symptoms of DKD mice and regulated these mice's blood glucose and lipid levels to some extent.

APL-based alleviation of renal injury in DKD mice

Twelve hours after the final administration, the renal function-related indicators were tested. Finally, a significant increase in the kidney index was monitored in the STZ group, indicating the occurrence of inflammation and impaired renal function in DKD mice. After being treated with APL, the mice showed a certain decrease in the kidney index, which denotes that the renal inflammation was eased (fig. 2A). As detected in the urine collected over 24 hours, the UAE of the STZ group increased. This suggests that the mice's glomerular filtration function was impaired. Meanwhile, the contents of Scr and BUN were heightened (P<0.05). These symptoms detected in urine were relieved following the APL intervention (figs. 2B-2D). It can be deduced that APL protected the kidneys of DKD mice somewhat.

As revealed by HE staining, the STZ group of mice had apparent glomerulosclerosis characterized by expanded glomerular mesangium along with cell proliferation, capillary collapse, and glomerular matrix deposition. However, these histopathological changes were notably improved in mice treated with APL (fig. 2E). Similar morphological change patterns were observed through PAS staining (fig. 2F). These consequences imply that APL can alleviate the STZ-induced renal pathological damage in mice.

APL-based amelioration of renal fibrosis in DKD mice

To ascertain the interference of APL in renal fibrosis, the expression of fibrotic proteins and pathological changes in renal tissues were examined in DKD mice treated with different doses of APL. After being administered with STZ, the mice exhibited greatly heightened levels of collagen I, TGF-β, α-SMA and fibronectin in the renal tissues; after being treated with APL, the mice underwent a sharp drop in the said levels proportionally to the dosage (P<0.05, figs. 3A-3B). This phenomenon explains that APL can restrain renal fibrosis and protect kidneys. Similar results were obtained through immunohistochemical staining of α-SMA in renal tissues (fig. 3C). Hence, APL may prevent mice from suffering renal tissue fibrosis induced by STZ.

APL-based relief of inflammation in DKD mice

Renal fibrosis may be connected with many pro-fibrotic and pro-inflammatory cytokines, involving such inflammatory factors as IL-6, IL-1β, and TNF-α. In this work, the expressions of inflammatory factors were examined by ELISA on the serum of DKD mice. The outcomes demonstrate that the levels of IL-1β, TNF-α, and IL-6 were highly elevated in mice (P<0.05) after being treated with STZ but were lowered in mice further treated with APL (figs. 4A-4C). The same results were acquired from western blot assays on the protein levels of inflammatory factors in the renal tissues of mice (figs. 4D-4E).

APL-based inhibition of the JNK/p38 signaling pathway

As reported (Long *et al.*, 2022), the MAPKs signaling pathway modulates the inflammatory responses and fibrosis in various organ tissues. Therefore, an evident rise was monitored in the phosphorylated protein levels of JNK, p38, and ERK in the MAPKs pathway after the mice were treated by STZ (P<0.05); after the mice were further administered with APL, a great dampening was examined in the phosphorylation levels of JNK and p38 but no great difference in the phosphorylated expression of ERK (P>0.05, figs. 5A-5D). Such findings prove that APL may exert its protective effects against DKD by stopping the activation of the JNK/p38 signaling pathway.

DISCUSSION

APL's potential impact on improving DKD remains uncertain, despite documented instances of APL's efficacy in reducing blood glucose levels in diabetic animal models (Jang *et al.*, 2017). In this work, the author discovered that APL extract, especially at a high dose (200mg/kg), significantly ameliorated the STZ-induced hyperglycemia and hyperlipidemia in DKD mice; it also effectively reduced the levels of serum creatinine, urinary albumin, serum urea nitrogen, and kidney index, improving the status of structural damage in kidneys. It was inferred that these changes might be caused by the pharmacological action of chemical components of APL (flavonoids, triterpenoids, phenols, etc.). Flavonoids, the main active components of APL, can inhibit oxidative stress and lessen pro-inflammatory factors, thereby improving podocyte damage, subsequently mitigating urinary micro albumin excretion and glomerular hyperfiltration and alleviating DKD (Vargas *et al.*, 2018; Liu *et al.*, 2024). Triterpenoids can suppress α-glucosidase, α-amylase, and aldose reductase to a large extent; they can enhance insulin secretion by activating TGR5 receptors, thereby improving glucose tolerance and regulating lipid metabolism; additionally, they can inhibit PTP1B to strengthen insulin sensitivity and normalize the blood glucose level (Roy *et al.*, 2024). Phenols in APL are primarily phloroglucin, which exhibits antioxidant and anti-inflammatory activities and can improve the endothelial function in hypertension (Hwang *et al.*, 2021); it can also protect pancreatic β-cells from glucose-induced apoptosis (Park and Han, 2015), thus mitigating diabetes and its complication, DKD damage. This study revealed for the first time the protective effect of APL in DKD mice.

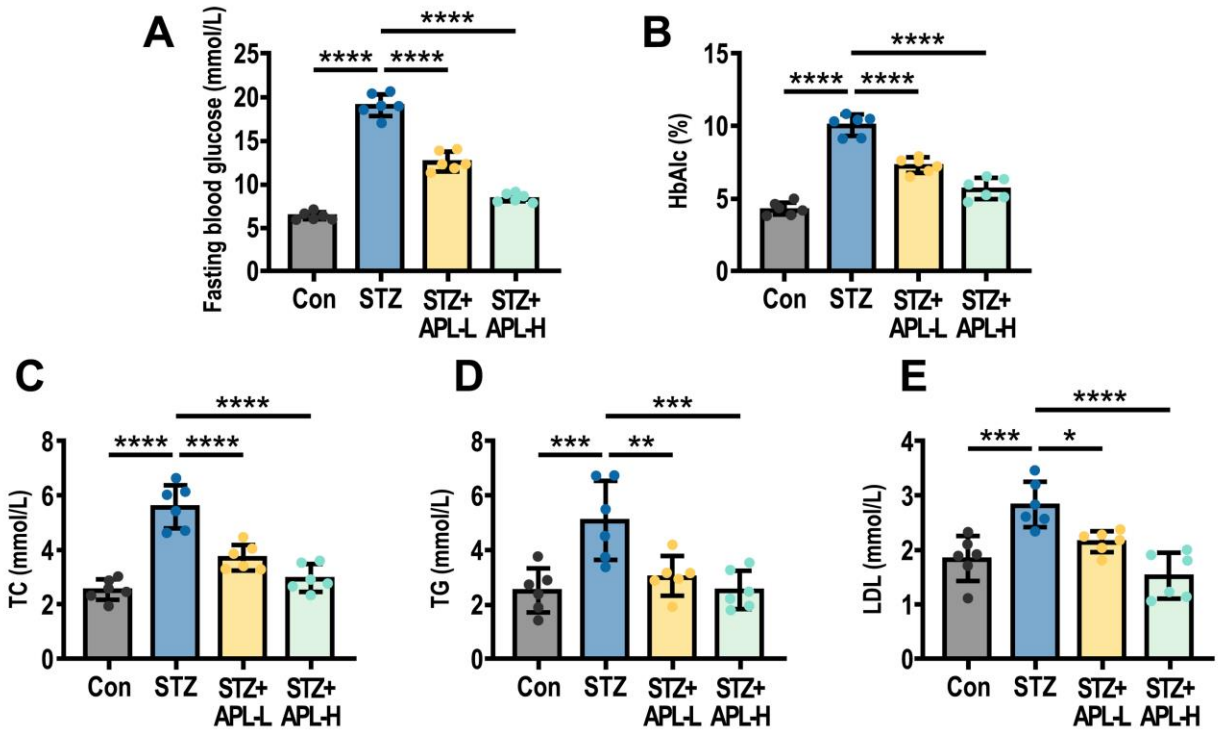

Fig. 1: APL-based improvement in the blood glucose and lipid levels of DKD mice (**P*<0.05, ***P*<0.01, ****P*<0.001, *****P*<0.0001). A: Levels of FBG in different groups; B: Levels of HbAlc in different groups; C: Levels of TC in different groups; D: Levels of TG in different groups; E: Levels of LDL in different groups.

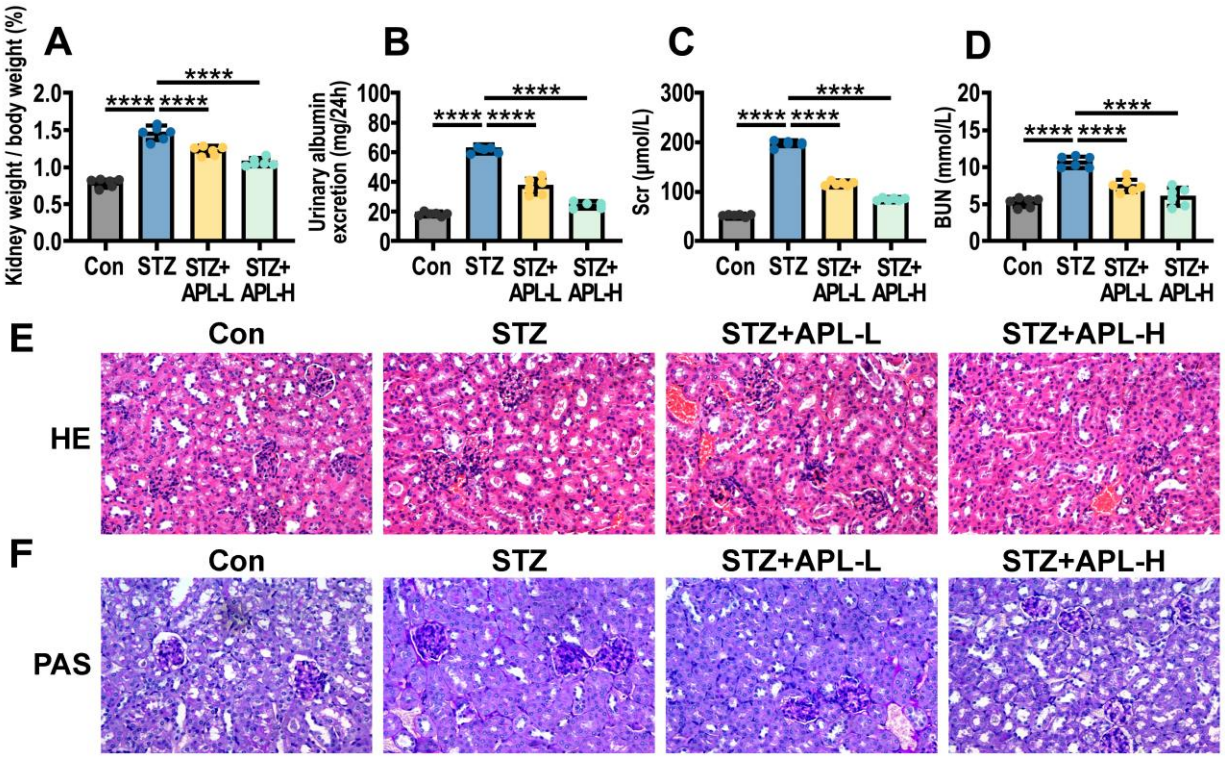

Fig. 2: APL-based alleviation of renal injury in DKD mice (*****P*<0.0001). A: Kidney index (kidney weight/body weight percentage); B: Urinary albumin (24-hour urine); C: Serum creatinine levels; D: Serum urea nitrogen levels; E: Kidney HE staining; F: Kidney PAS staining.(The red, green, yellow, and blue arrows represent vascular collapse, matrix deposition, thickened tethered dilation, and cell proliferation, respectively. Scale 40×50 μm)

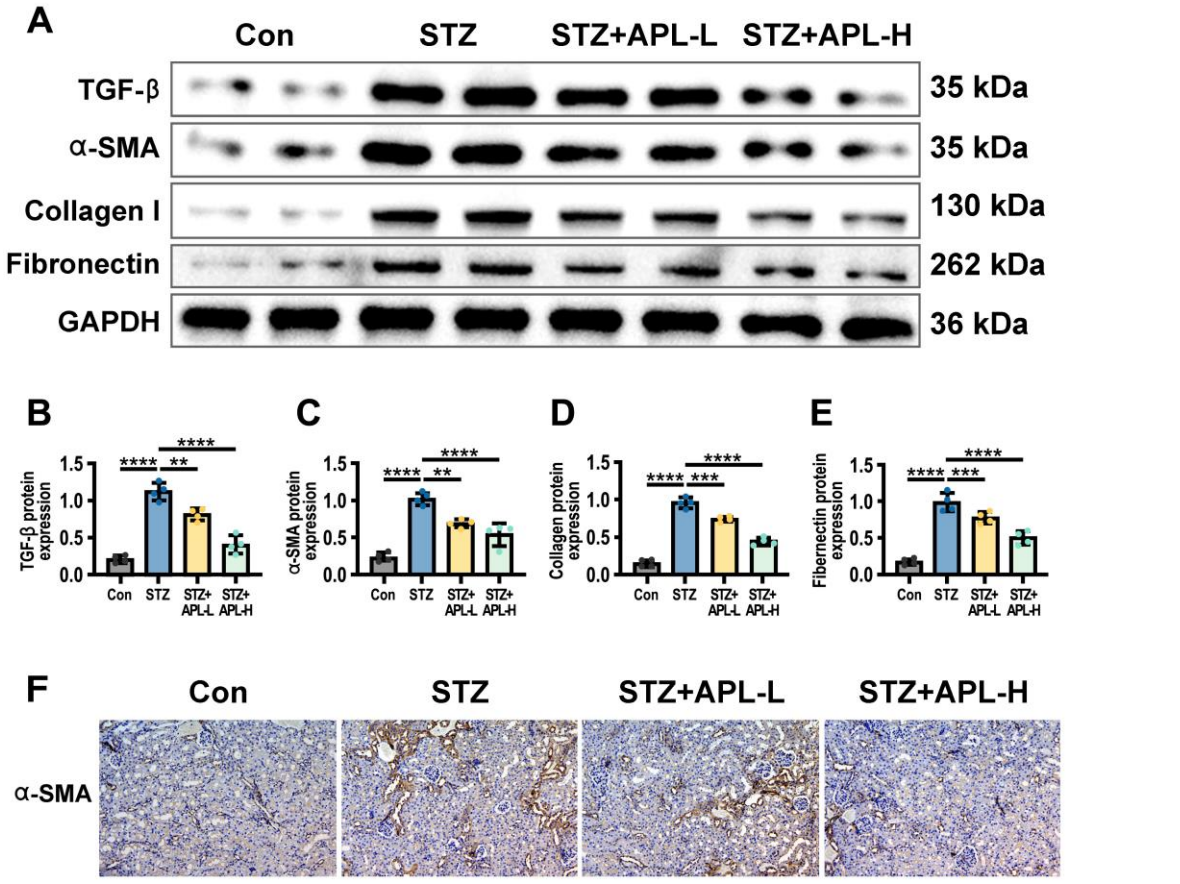

Fig. 3: APL-based amelioration of renal fibrosis in DKD mice (****P<0.0001). A/B: Expression of fibrotic proteins in renal tissues; C: Immunohistochemical staining of α-SMA in renal tissues, Scale 40×50 μm.

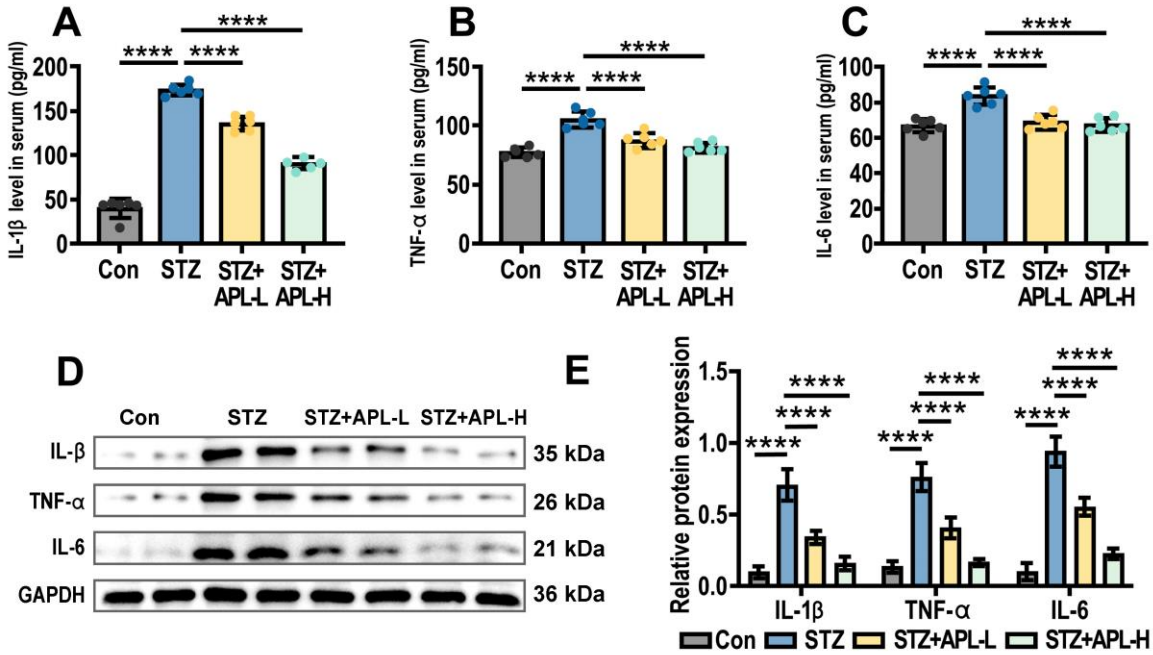

Fig. 4: APL-based relief of inflammation in DKD mice (****P<0.0001). A: Levels of IL-1β in different groups; B: Levels of TNF-α in different groups; C: Levels of IL-6 in different groups; D/E: Protein expression of inflammatory factors in renal tissues.

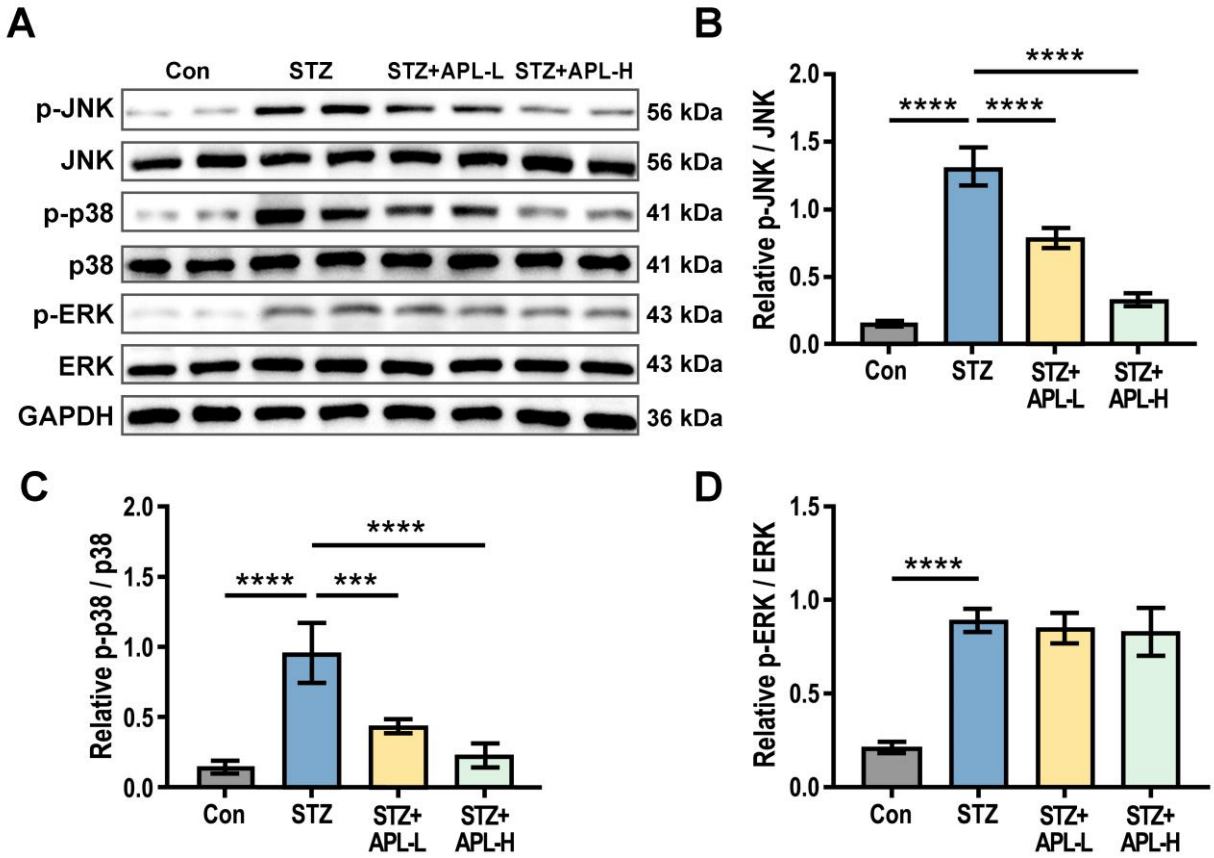

Fig. 5: APL-based inhibition of the JNK/p38 signaling pathway (****P<0.0001). A: Expression of proteins in the JNK/p38 pathway; B/C/D: Protein quantification diagram.

Notably, tissue fibrosis is the result of repeated wound healing and tissue remodeling. It is typically attributed to chronic inflammation caused by epithelial damage. Many pro-inflammatory factors such as IL-6, IL-1β, and TNF-α play crucial parts in early excessive inflammatory responses during tissue fibrosis of an organ (Amir and Czaja, 2018). As demonstrated in published articles, IL-1β contributes to the onset of tubulointerstitial disorders by inducing injury and fibrosis in proximal renal tubules (Otto, 2018), TNF-α facilitates tissue remodeling by stimulating the accumulation of inflammatory mediators and cytokines and further promoting myofibroblasts to differentiate and synthesize into the extra cellular matrix (Gamad *et al.*, 2018), the role of IL-6 in intensifying both wound healing and fibrotic reactions is notable, and its ablation could weaken the fibrosis of kidneys in mice (Chen *et al.*, 2019). TGF-β, as a key inflammatory cytokine that fosters fibrosis, significantly contributes to glomerulosclerosis and interstitial fibrosis in various renal pathologies encompassing DKD. If TGF-β becomes abnormal under a high blood sugar level, extra cellular matrix proteins (collagen and fibronectin) may accumulate excessively, causing thickened glomerular basement membrane and expanded mesangium (Wang *et al.*, 2015). The excessively accumulated extra cellular matrix can trigger renal fibrosis and activate fibroblasts, specifically manifesting as increased secretion of α-SMA, collagen I, and fibronectin (He *et al.*, 2022). In this survey, compared to mice in the control group, the STZ-induced mice showed elevated expression of IL-1β, TNF-α, IL-6, TGF-β, α-SMA, collagen I and fibronectin in renal tissue. This phenomenon reveals that renal fibrosis was aggravated. However, this phenomenon was alleviated largely with the administration of APL, reducing renal damage in DKD mice.

MAPKs, composed of ERK, JNK, and p38 MAPK routes, are pivotal in the process of inflammation and fibrosis (Yoshida *et al.*, 2002; Cargnello and Roux, 2011). As reported, fibroblasts can split into myofibroblasts, and the hyperphosphorylation of JNK is closely connected with tissue fibrosis (Yoshida *et al.*, 2002); during the progression of DKD, the activation of the p38 MAPK pathway mediates the expression of collagen and fibrous protein induced by TGF-β (Choi *et al.*, 2012); the activation of such signaling molecules as ERK and p38 MAPK dominates inflammation as well as renal fibrosis (Hagiwara *et al.*, 2006; Cargnello and Roux, 2011). As monitored in this work, APL lessened the phosphorylation of JNK and p38 but posed no large impact on the

phosphorylation level of ERK. This outcome proves that APL can ameliorate the state of renal tissue fibrosis in DKD mice by restraining the JNK/p38 pathway.

CONCLUSION

In summary, APL may prevent renal tissue fibrosis and further alleviate DKD by dampening the inflammatory response mediated by the JNK/p38 MAPK signaling pathway. Therefore, APL emerges as a promising alternative medication for the clinical treatment of DKD.

REFERENCES

Ahmad J (2015). Management of diabetic nephropathy: Recent progress and future perspective. *Diabetes Metab. Syndr.*, **9**(4): 343-58.

Amir M and Czaja MJ (2018). Inflammasome-mediated inflammation and fibrosis: It is more than just the IL-1beta. *Hepatology*, **67**(2): 479-481.

Bae H, Kim HJ, Shin M, Lee H, Yin CS, Ra J and Kim J (2010). Inhibitory effect of *Agrimoniae herba* on lipopolysaccharide-induced nitric oxide and proinflammatory cytokine production in BV2 microglial cells. *Neurol. Res.*, **32**(Suppl 1): 53-57.

Cargnello M and Roux PP (2011). Activation and function of the MAPKs and their substrates, the MAPK-activated protein kinases. *Microbiol Mol Biol Rev.*, **75**(1): 50-83.

Chen W, Yuan H, Cao W, Wang T, Chen W, Yu H, Fu Y, Jiang B, Zhou H, Guo H and Zhao X (2019). Blocking interleukin-6 trans-signaling protects against renal fibrosis by suppressing STAT3 activation. *Theranostics*, **9**(14): 3980-3991.

Choi ME, Ding Y and Kim SI (2012). TGF-beta signaling via TAK1 pathway: Role in kidney fibrosis. *Semin Nephrol*, **32**(3): 244-252.

Gamad N, Malik S, Suchal K, Vasisht S, Tomar A, Arava S, Arya DS and Bhatia J (2018). Metformin alleviates bleomycin-induced pulmonary fibrosis in rats: Pharmacological effects and molecular mechanisms. *Biomed Pharmacother.*, **97**: 1544-1553.

Hagiwara S, Makita Y, Gu L, Tanimoto M, Zhang M, Nakamura S, Kaneko S, Itoh T, Gohda T, Horikoshi S and Tomino Y (2006). Eicosapentaenoic acid ameliorates diabetic nephropathy of type 2 diabetic KKAy/Ta mice: involvement of MCP-1 suppression and decreased ERK1/2 and p38 phosphorylation. *Nephrol Dial Transplant*, **21**(3): 605-15.

He M, Feng L, Chen Y, Gao B, Du Y, Zhou L, Li F and Liu H (2022). Polydatin attenuates tubulointerstitial fibrosis in diabetic kidney disease by inhibiting YAP expression and nuclear translocation. *Front Physiol.*, **13**: 927794.

Hwang J, Yang HW, Lu YA, Je JG, Lee HG, Fernando KHN, Jeon YJ and Ryu B (2021). Phloroglucinol and dieckol isolated from *Ecklonia cava* suppress impaired diabetic angiogenesis; A study of in-vitro and in-vivo. *Biomed Pharmacother*, **138**: 111431.

Jang HH, Nam SY, Kim MJ, Kim JB, Choi JS, Kim HR and Lee YM (2017). *Agrimonia pilosa* Ledeb. aqueous extract improves impaired glucose tolerance in high-fat diet-fed rats by decreasing the inflammatory response. *BMC Complement. Altern. Med.*, **17**(1): 442.

Jin T, Chi L and Ma C (2022). *Agrimonia pilosa*: A phytochemical and pharmacological review. *Evid. Based Complement. Alternat. Med.*, p.3742208.

Jin X, Song S, Wang J, Zhang Q, Qiu F and Zhao F (2016). Tiliroside, the major component of *Agrimonia pilosa* Ledeb. ethanol extract, inhibits MAPK/JNK/p38-mediated inflammation in lipopolysaccharide-activated RAW 264.7 macrophages. *Exp. Ther. Med.*, **12**(1): 499-505.

Johnson SA and Spurney RF (2015). Twenty years after ACEIs and ARBs: Emerging treatment strategies for diabetic nephropathy. *Am. J. Physiol. Renal Physiol.*, **309**(10): F807-F820.

Jung CH, Kim JH, Park S, Kweon DH, Kim SH and Ko SG (2010). Inhibitory effect of *Agrimonia pilosa* Ledeb. on inflammation by suppression of iNOS and ROS production. *Immunol. Invest.*, **39**(2): 159-70.

Kim CY, Yu QM, Kong HJ, Lee JY, Yang KM and Seo JS (2020). Antioxidant and anti-inflammatory activities of *Agrimonia pilosa* Ledeb. extract. *Evid. Based Complement. Alternat. Med.*, p.8571207.

Kim SB, Hwang SH, Suh HW and Lim SS (2017). Phytochemical analysis of *Agrimonia pilosa* Ledeb, its antioxidant activity and aldose reductase inhibitory potential. *Int. J. Mol. Sci.*, **18**(2): 379.

Liu PY, Hong KF, Liu YD, Sun ZY, Zhao TT, Li XL, Lao CC, Tan SF, Zhang HY, Zhao YH, Xie Y and Xu YH (2024). Total flavonoids of Astragalus protects glomerular filtration barrier in diabetic kidney disease. *Chin. Med.*, **19**(1): 27.

Long Y, Niu Y, Liang K and Du Y (2022). Mechanical communication in fibrosis progression. *Trends Cell Biol.*, **32**(1): 70-90.

Otto G (2018). IL-1beta switches on kidney fibrosis. *Nat. Rev. Nephrol.*, **14**(8): 475.

Park MH and Han JS (2015). Phloroglucinol Protects INS-1 pancreatic beta-cells against glucotoxicity-induced apoptosis. *Phytother. Res.*, **29**(11): 1700-1706.

Perez-Morales RE, Del Pino MD, Valdivielso JM, Ortiz A, Mora-Fernandez C and Navarro-Gonzalez JF (2019). Inflammation in diabetic kidney disease. *Nephron*, **143**(1): 12-16.

Piccoli GB, Grassi G, Cabiddu G, Nazha M, Roggero S, Capizzi I, De Pascale A, Priola AM, Di Vico C, Maxia S, Loi V, Asunis AM, Pani A and Veltri A (2015). Diabetic kidney disease: A syndrome rather than a single disease. *Rev. Diabet. Stud.*, **12**(1-2): 87-109.

Roy S, Ghosh A, Majie A, Karmakar V, Das S, Dinda SC, Bose A and Gorain B (2024). Terpenoids as potential phytoconstituent in the treatment of diabetes: From

preclinical to clinical advancement. *Phytomedicine*, **129**: 155638.

Samsu N (2021). Diabetic nephropathy: Challenges in pathogenesis, diagnosis and treatment. *Biomed. Res. Int.*, **2021**: 1497449.

Sanchez AP and Sharma K (2009). Transcription factors in the pathogenesis of diabetic nephropathy. *Expert Rev. Mol. Med.*, **11**: e13.

Santos TN, Costa G, Ferreira JP, Liberal J, Francisco V, Paranhos A, Cruz MT, Castelo-Branco M, Figueiredo IV and Batista MT (2017). Antioxidant, anti-inflammatory and analgesic activities of *Agrimonia eupatoria* L. infusion. *Evid. Based Complement. Alternat. Med.*, **2017**: 8309894.

Tang G, Li S, Zhang C, Chen H, Wang N and Feng Y (2021). Clinical efficacies, underlying mechanisms and molecular targets of Chinese medicines for diabetic nephropathy treatment and management. *Acta Pharm. Sin. B*, **11**(9): 2749-2767.

Vargas F, Romecin P, Garcia-Guillen AI, Wangesteen R, Vargas-Tendero P, Paredes MD, Atucha NM and Garcia-Estan J (2018). Flavonoids in kidney health and disease. *Front Physiol*, **9**: 394.

Wang T, Chen SS, Chen R, Yu DM and Yu P (2015). Reduced beta 2 glycoprotein I improves diabetic nephropathy via inhibiting TGF-beta1-p38 MAPK pathway. *Int. J. Clin. Exp. Pathol.*, **8**(3): 2321-33.

Wen S, Zhang X, Wu Y, Yu S, Zhang W, Liu D, Yang K and Sun J (2022). *Agrimonia pilosa* Ledeb.: A review of its traditional uses, botany, phytochemistry, pharmacology, and toxicology. *Heliyon*, **8**(8): e09972.

Yoshida K, Kuwano K, Hagimoto N, Watanabe K, Matsuba T, Fujita M, Inoshima I and Hara N (2002). MAP kinase activation and apoptosis in lung tissues from patients with idiopathic pulmonary fibrosis. *J. Pathol.*, **198**(3): 388-396.

Zhang B, Zhang X, Zhang C, Sun G and Sun X (2021). Berberine improves the protective effects of metformin on diabetic nephropathy in db/db Mice through Trib1-dependent Inhibiting Inflammation. *Pharm. Res.*, **38**(11): 1807-1820.

Zhang Y, Sun Y, Peng R, Liu H, He W, Zhang L, Peng H and Zhang Z (2018). The long noncoding RNA 150Rik promotes mesangial cell proliferation via miR-451/IGF1R/p38 MAPK signaling in diabetic nephropathy. *Cell Physiol Biochem.*, **51**(3): 1410-1428.